



1 Laboratory and field evaluation of the Aerosol Dynamics Inc. concentrator (ADIC)  
2 for aerosol mass spectrometry

3

4 Sanna Saarikoski<sup>1</sup>, Leah R. Williams<sup>2</sup>, Steven R. Spielman<sup>3</sup>, Gregory S. Lewis<sup>3</sup>, Arantzazu  
5 Eiguren-Fernandez<sup>3</sup>, Minna Aurela<sup>1</sup>, Susanne V. Hering<sup>3</sup>, Kimmo Teinilä<sup>1</sup>, Philip Croteau<sup>2</sup>, John  
6 T. Jayne<sup>2</sup>, Thorsten Hohaus<sup>2,+</sup>, Douglas R. Worsnop<sup>2</sup>, Hilikka Timonen<sup>1</sup>

7

8 <sup>1</sup> Atmospheric Composition Research, Finnish Meteorological Institute, Helsinki, Finland

9 <sup>2</sup> Center for Aerosol and Cloud Chemistry, Aerodyne Research, Inc., Billerica, MA, USA

10 <sup>3</sup> Aerosol Dynamics Inc., Berkeley, CA, USA

11 <sup>+</sup> Now at Institute of Energy and Climate Research, IEK-8: Troposphere, Forschungszentrum

12 Juelich GmbH, Juelich, Germany

13



14 **Abstract**

15 An air-to-air ultrafine particle concentrator (Aerosol Dynamics Inc. concentrator; ADIc) has been  
16 designed to enhance on-line chemical characterization of ambient aerosols by aerosol mass  
17 spectrometry. The ADIc employs a three-stage, moderated water-based condensation growth tube  
18 coupled to an aerodynamic focusing nozzle to concentrate ultrafine particles into a portion of the  
19 flow. The system can be configured to sample between 1.0–1.7 L min<sup>-1</sup> with an output concentrated  
20 flow between 0.08–0.12 L min<sup>-1</sup>, resulting in a theoretical concentration factor (sample flow/output  
21 flow) ranging from 8 to 21. Laboratory tests with monodisperse particles show that the ADIc is  
22 effective for particles as small as 10 nm. Laboratory experiments conducted with the Aerosol Mass  
23 Spectrometer (AMS) showed no shift in the particle size after the ADIc, as measured by the AMS  
24 particle time-of-flight. The ADIc-AMS system was operated unattended over a one-month period  
25 near Boston, Massachusetts. Comparison to a parallel AMS without the concentrator showed  
26 concentration factors of  $9.7 \pm 0.15$  and  $9.1 \pm 0.1$  for sulfate and nitrate, respectively, when operated  
27 with a theoretical concentration factor of  $10.5 \pm 0.3$ . Concentration factor of organics was lower,  
28 possibly due to the presence of large particles from nearby road-paving operations, and a difference  
29 in aerodynamic lens cutoff between the two AMS instruments. Another field deployment was  
30 carried out in Helsinki, Finland. Two ~10-day measurement periods showed good correlation for  
31 the concentrations of organics, sulfate, nitrate and ammonium measured with an Aerosol Chemical  
32 Speciation Monitor (ACSM) after the ADIc, and a parallel AMS without the concentrator.  
33 Additional experiments with an AMS alternating between the ADIc and a bypass line  
34 demonstrated that the concentrator did not change the size distribution or the chemistry of the  
35 ambient aerosol particles.

36



## 37 **1 Introduction**

38 Particles in the ambient atmosphere are of concern for human health, air quality and climate change  
39 (Pope and Dockery, 2006; Lelieveld et al., 2015; IPCC 2014). Measurement of the chemical  
40 characteristics of particles, and the health effects associated with their inhalation, often benefit  
41 from higher sample load which can be achieved by increasing sample flow rate, extending  
42 sampling time or using a particle concentrator. Enrichment of particle number or mass  
43 concentration is particularly important for measurements in regions where particle concentrations  
44 are low, such as in Arctic or Antarctic background areas (10–1000 particles per cm<sup>-3</sup>, Asmi et al.,  
45 2010; Tunved et al., 2006). An increase in particle mass can also benefit the measurement of trace  
46 aerosol components such as metals, or improve the determination of chemically resolved size  
47 distributions.

48 Several air-to-air concentrators have been designed to increase the concentration of particles with  
49 respect to the suspending gas volume, and to thereby providing enhanced aerosol detection. To be  
50 beneficial, the concentrator should be small, easy to maintain and capable of operating several  
51 days or even weeks unattended. Even more importantly, the concentrator should provide stable  
52 enrichment of particles, and maintain aerosol chemical and physical and properties such as  
53 composition and size distribution. Virtual impactors are a well-known type of air-to-air particle  
54 concentrators that use a low-velocity sampling probe to sample a particle flow exiting from a  
55 nozzle but they are typically ineffective for the submicrometer (< 1 µm) and ultrafine (< 100 nm)  
56 particle size ranges that are of most interest for atmospheric and health-related particle studies.  
57 Current air-to-air concentrators for small particles couple condensational growth with traditional  
58 virtual impactors, e.g., the Versatile Aerosol Concentration Enrichment System (VACES, Kim et  
59 al., 2001), the miniature VACES (Geller et al., 2006; Saarikoski et al., 2014) or the Harvard  
60 Ultrafine Concentrated Ambient Particle System (HUCAPS, Gupta et al., 2004). However, these  
61 systems are ineffective for particles below ~30 nm in diameter. Moreover, with long  
62 condensational growth times, these approaches have been shown to feature the undesirable effect  
63 of changing the particle chemical composition (e.g., Saarikoski et al., 2014).

64 Here we present a new air-to-air particle concentrator, the Aerosol Dynamics Inc. concentrator  
65 (ADIC), that is based on the three-stage, laminar-flow, water-based condensational growth  
66 approach used in the Sequential Spot Sampler (Eiguren Fernandez et al., 2014; Pan et al., 2016),



67 and in some water condensation particle counters (CPCs, Hering et al., 2017; 2018). This system  
68 is designed specifically for instruments with low sampling flow rates on the order of  $0.1 \text{ L min}^{-1}$ .  
69 It offers concentration factors (CFs) of 8 to 21 for particles as small as 10 nm diameter in an output  
70 flow that is noncondensing at typical room temperatures (i.e. with dew points below  $16 \text{ }^\circ\text{C}$ ).  
71 Previously, a preliminary version of this concentration approach that used a two-stage growth tube  
72 was coupled to an Aerosol Time-of-Flight Mass Spectrometer (ATOFMS, Zauscher et al., 2011)  
73 and showed both concentration enhancement and lack of chemical artifacts. However, this  
74 preliminary system was not stable enough for long-term operation.

75 The three-stage growth column version of the ADIc described here eliminates excess water vapor  
76 in the output flow and decreases the residence time for the particle in the droplet phase, with the  
77 objective of minimizing chemical artifacts as well as providing long-term stability. The ADIc is a  
78 smaller scaled version of the approach used in the nano-particle charger reported by Kreisberg et  
79 al. (2018), for which chemical artifacts, evaluated using Thermal Desorption Chemical Ionization  
80 Mass Spectrometry, were found to be mostly insignificant. The ADIc is tailored for use with an  
81 aerosol mass spectrometer, such as the Aerodyne Aerosol Mass Spectrometer (AMS) or ATOFMS.  
82 In this paper, the ADIc was evaluated in laboratory experiments that explored its influence on  
83 particle size and chemical composition. The ADIc was also evaluated in field measurements  
84 conducted in two different environments (urban and urban background) and with different  
85 commonly used types of aerosol mass spectrometers. Moreover, long term (weeks to months)  
86 unattended operation of the ADIc was demonstrated.

87

## 88 **2 Experimental**

### 89 **2.1 System description of the ADIc**

90 The ADIc uses a laminar flow, water- based condensation growth tube coupled to an aerodynamic  
91 focusing nozzle to provide concentration of particles from a  $1\text{--}1.7 \text{ L min}^{-1}$  sample flow into a  $0.08\text{--}$   
92  $0.12 \text{ L min}^{-1}$  concentrated output flow. This system uses a three-stage moderated aerosol  
93 condensation approach (Hering et al., 2014) whereby the aerosol flow passes through a wet-walled  
94 tube with three distinct temperature regions (Fig. 1). In the first stage, the conditioner has cold  
95 walls and brings the flow to known conditions of cool temperature and high relative humidity  
96 (RH). The second, initiator stage, has warm walls and provides the water vapor that creates the



97 supersaturation for particle activation, while the last, cool-walled moderator stage provides time  
98 for particle growth while simultaneously removing water vapor from the flow. The water vapor  
99 saturation level reaches a value of 1.4 in the initiator while maintaining temperatures below 30 °C  
100 in the majority of the sample flow, and simultaneously providing for output flow dew points below  
101 16 °C. Thus, the water vapor content of the output flow is reduced to typical ambient conditions,  
102 making it easier to handle, and minimizing the amount of water reaching the detection system. The  
103 wetted walls are maintained by a single wick formed from rolled membrane filter media and the  
104 flow is laminar throughout the ADIc system.

105 Within the growth tube, particles with diameters above 5–10 nm are activated and grow by  
106 condensation to form droplets of approximately 1.5–4 μm in diameter. The cooled, droplet-laden  
107 flow passes through a 1-mm diameter nozzle wherein the droplets are aerodynamically focused  
108 along the central core of the flow, much as described by Fuerstenau et al. (1994). The ADIc  
109 contains an annular slit in the side wall of this nozzle, through which the majority (85–95 %) of  
110 the flow (discard flow) is extracted. The remaining 5–15 % of the flow contains the droplets which  
111 have been focused aerodynamically. Water evaporates from the droplets once the flow regains  
112 ambient (20–25 °C) temperature to provide a concentrated aerosol flow (output flow). The system  
113 is designed to minimize the time the particle is a droplet, with the objective of minimizing chemical  
114 artifacts, similar to the nano-particle charging system (Kreisberg et al., 2018).

115 The exact design of the focusing and flow extraction nozzle is based on numerical modeling done  
116 using the Comsol Multiphysics package. Numerical modeling results, presented in Fig. S1 for the  
117 final design, show that particles smaller than 1 μm follow the gas flow trajectories and are extracted  
118 through the annular slit while those above 6 μm over-focus and collide with the opposite wall.  
119 However, intermediately sized particles, corresponding to a Stokes number (St) of 0.5 to 3.5, are  
120 aerodynamically focused in the region near the centerline of the flow. These particles follow the  
121 remaining flow, the output flow, which continues straight, thus providing a concentrated flow for  
122 sampling with aerosol instrumentation. The theoretical concentration factor is determined by the  
123 ratio of the sample flow rate to the output flow rate and can be varied between 8 and 21.

124 Two prototype concentrators (Prototype 1 and 2) were used in this study, both having the same  
125 dimensions for the growth tube and nozzle. The conditioner, initiator and moderator are 140 mm,  
126 51 mm and 102 mm long, respectively, separated by 7.5 mm thick insulator sections. In both



127 prototypes the growth tube was lined with a 9 mm-ID, ~1.5 mm-thick wick formed from rolled  
128 membrane filter. The conditioner and moderator were cooled using Peltier heat pumps and the  
129 initiator and focusing nozzle were heated resistively. All three regions used proportional-integral-  
130 derivative (PID) control to maintain set-point temperatures. Distilled water was injected into the  
131 initiator stage at a rate of  $5 \mu\text{L min}^{-1}$  and excess water was removed from the base of the wick  
132 carried by a small flow of  $\sim 0.05 \text{ L min}^{-1}$  of air into a waste bottle. Other than packaging, the only  
133 difference between the prototypes was that Prototype 1 had a mass flow meter to measure the  
134 discard flow while Prototype 2 did not have this option. The theoretical CF for Prototype 1 was  
135 determined continuously from the measured flows, while for Prototype 2 the theoretical CF was  
136 determined from the sample and concentrated flow rates measured before and after each  
137 experiment. The size of the ADIc is approximately 30 x 30 x 50 cm (W x D x H) and the weight  
138 is  $\sim 11 \text{ kg}$ .

139

## 140 **2.2 Evaluation in the laboratory**

### 141 **2.2.1 Particle number measurements at ADI**

142 The performance of the ADIc for particle counting was evaluated in the laboratory at Aerosol  
143 Dynamics Inc. (ADI) using monodisperse particles generated by atomization, followed by drying  
144 and charge conditioning (soft X-ray, Model 3087, TSI Inc., Shoreview, US). Particles were size  
145 selected using a nano-differential mobility analyzer (DMA, Model 3085, TSI Inc., Shoreview, US)  
146 for sizes between 5 nm and 60 nm and using the Aerosol Dynamics Inc. high-flow DMA  
147 (Stolzenburg et al., 1998) for sizes between 20 nm and 600 nm. Particle concentrations were  
148 measured in the sample flow and in the concentrated output flow using water-based CPCs.  
149 Prototype 1 was evaluated with mono-mobility ammonium sulfate (AS) particles with a pair of  
150 prototype Model 3785 (TSI Inc., Shoreview, US) water-based CPCs and a Model 3783 CPC (TSI  
151 Inc., Shoreview, US) to simultaneously measure particle concentrations in the sample flow, in the  
152 discard flow, and in the concentrated output flow, respectively. The sample flow was fixed at  $1.0$   
153  $\text{L min}^{-1}$ , and the output flow was  $0.12 \text{ L min}^{-1}$  (theoretical CF = 8.3). The operating temperatures  
154 for conditioner (Tcon), initiator (Tini), moderator (Tmod) and focusing nozzle (Tnoz) were 5, 26,  
155 10 and 30 °C, respectively (see Table 1).



156 Similar evaluation experiments were carried out on Prototype 2 but its operation was tested under  
157 two flow regimes. First, experiments were done at  $1.0 \text{ L min}^{-1}$  sample flow and  $0.11 \text{ L min}^{-1}$  output  
158 flow (theoretical CF = 9.1), with similar operating temperatures to Prototype 1. To test higher CFs,  
159 experiments were also done at a sample flow rate of  $1.5 \text{ L min}^{-1}$  and an output flow of  $0.11$   
160  $\text{L min}^{-1}$  for a theoretical CF of 13.6. The growth tube is sized for low-flow operation, such that the  
161 centerline supersaturation reaches its maximum at the end of the warm initiator section. At the  
162 higher flow rate, the residence time is shorter, and thus for the same operating temperatures the  
163 peak supersaturation is lower. To compensate, the initiator was operated at a warmer wall  
164 temperature, thereby providing a similar value for the calculated peak super-saturation. The  
165 operating temperatures for the high flow were  $T_{\text{con}} = 6 \text{ }^{\circ}\text{C}$ ,  $T_{\text{ini}} = 31 \text{ }^{\circ}\text{C}$ ,  $T_{\text{mod}} = 8 \text{ }^{\circ}\text{C}$ , and  $T_{\text{noz}}$   
166  $= 35 \text{ }^{\circ}\text{C}$  (Table 1).

167 In addition to laboratory generated AS particles, both prototypes were tested with laboratory air  
168 using a pair of water-based CPCs, one sampling upstream of the ADIC and one sampling  
169 downstream.

170

### 171 **2.2.2 Particle chemistry at ARI and FMI**

172 The performance of the ADIC in terms of particle chemistry was evaluated at Aerodyne Research,  
173 Inc. (ARI) and at the Finnish Meteorological Institute (FMI). Laboratory experiments were carried  
174 out by using particles generated with a constant output atomizer (Model 3076, TSI Inc., Shoreview,  
175 US) from AS or ammonium nitrate (AN) in deionized water, or from dioctyl sebacate (DOS) in 2-  
176 propanol. Generated particles were dried with a silica gel dryer and the desired monodisperse  
177 particle size fraction was selected using a DMA (Model 3080, TSI Inc., Shoreview, US). A valve  
178 system was used to alternate between passing the particles through the ADIC and bypassing it.  
179 Temperature and flow settings used in the ADIC during the ARI and FMI experiments are given  
180 in Table 1.

181 Particle size and chemical composition were measured with several different versions of the AMS,  
182 including a high-resolution time-of-flight aerosol mass spectrometer (HR-AMS, Aerodyne  
183 Research Inc., Billerica, US; DeCarlo et al., 2006), a soot-particle aerosol mass spectrometer (SP-  
184 AMS, Aerodyne Research Inc., Billerica, US; Onasch et al., 2012), a quadrupole aerosol mass



185 spectrometer (Q-AMS, Aerodyne Research Inc., Billerica, US; Canagaratna et al., 2007) and a  
186 quadrupole aerosol chemical speciation monitor (ACSM, Aerodyne Research Inc., Billerica, US;  
187 Ng et al., 2011). These instruments all operate on the same principle. Aerosol particles are sampled  
188 through an aerodynamic lens, forming a narrow particle beam that is transmitted into the detection  
189 chamber where the non-refractory species are flash vaporized upon impact on a hot surface (600  
190 °C). The particle vapor is ionized using electron impact ionization (70 eV) and detected by the  
191 mass spectrometer. Particle size (particle time of flight (PToF) data) is determined from particle  
192 flight time in the vacuum chamber after passing through a chopper. The typical size range of  
193 particles detected with an AMS is 70 nm to 700 nm (Liu et al., 2007). In addition to the thermal  
194 vaporizer, the SP-AMS incorporates an intracavity Nd-YAG (1064 nm) laser that enables the  
195 determination of refractory black carbon (rBC) and metal containing particles (Onasch et al., 2012;  
196 Carbone et al., 2015). The ACSM does not include particle size measurement capability.

197 HR- and SP-AMS data was analyzed with the Squirrel (v1.57H)/Pika (v1.16H) and Squirrel  
198 (v1.60P)/Pika (v1.20P) analysis package, respectively. Additionally, high resolution (HR) size  
199 distribution data from the SP-AMS was analyzed with Squirrel (v1.62A)/Pika (v1.22A) package.  
200 Both the HR-AMS and SP-AMS instruments were equipped with a multiplex chopper and the  
201 measured size distributions were normalized to the mass spectra. Q-AMS data was analyzed with  
202 AMS Analysis Toolkit 1.43. ACSM data was analyzed with ACSM Local (v1.6.1.1). All of the  
203 analysis software runs in the Igor 6 (WaveMetrics, Inc.) programming environment. The three  
204 AMS instruments and the ACSM were calibrated for ionization efficiency (IE) of nitrate and  
205 relative ionization efficiency (RIE) of both ammonium and sulfate, using size selected single  
206 component particles of AN or AS (Budisulistiorini et al., 2014).

207

### 208 **2.3 Field testing**

209 The ADIC was tested for ambient aerosol at two different locations. At ARI, particles were sampled  
210 from a roof top sampling station on the ARI building at 45 Manning St., Billerica, MA (42.53, -  
211 71.27, 60 m a.s.l.), located about 60 m NE of a major freeway. Ambient air was sampled at 3 L  
212 min<sup>-1</sup> through a 2.5 µm cut cyclone and split between two paths. The first path went to an HR-  
213 AMS and a CPC (Model 3776, TSI Inc., Shoreview, US). The second path went to the ADIC  
214 followed by a Q-AMS and a CPC (Model mCPC, Brechtel, Hayward, US). Two valves allowed





215 the ambient air to bypass the ADIc and directly enter the Q-AMS. Both AMSs recorded data at 2-  
216 minute time resolution. Ambient sampling was conducted from 1 to 26 August 2014. The default  
217 collection efficiency (CE) of 0.5 for ambient particles was applied to data from both AMS  
218 instruments. Local ambient temperature was downloaded from Weather Underground for station  
219 KMABILLE10 and ambient RH data was downloaded from NOAA for Hanscom.

220 The second ambient sampling location was at an urban background station (SMEARIII; Station  
221 for Measuring Ecosystem-Atmosphere Relationships, 60.20, 24.95, 30 m a.s.l., described by Järvi  
222 et al., 2009) located at the Kumpula campus near the FMI building, about 5 km NE of the Helsinki  
223 city center, Finland. The station is surrounded by office buildings on one side and a small forest  
224 and botanical garden on the other side. Ambient particles were sampled through a 2.5  $\mu\text{m}$  cyclone  
225 with a flow rate of 3 L  $\text{min}^{-1}$ . Sample flow was split into two sampling lines; the first line went to  
226 the SP-AMS (with an additional bypass flow of 1.3–2 L  $\text{min}^{-1}$ ) and the second line to the ADIc  
227 followed by an ACSM. The ACSM data was averaged approximately to 10-minute time resolution  
228 (10 times open + close, m/z range: 10–150, scan rate 200 ms/amu) and the SP-AMS measured  
229 with a time resolution of 1.5 minutes. Two sample flow regimes were tested with the ACSM+ADIc  
230 system; the sample flow was set to either 1.7 L  $\text{min}^{-1}$  or 1.0 L  $\text{min}^{-1}$  while the output flow of the  
231 ADIc was determined by the ACSM inlet flow of 0.08 L  $\text{min}^{-1}$ , giving a theoretical CF of 21.3 and  
232 12.5 for high and low sample flow, respectively. Additionally, in a separate set of experiments, the  
233 ADIc was installed upstream of the SP-AMS in order to investigate the influence of the ADIc on  
234 high resolution mass spectra and size distributions. Those tests were carried out in the high flow  
235 regime (theoretical CF of 21.3) in order to maximize the increase in HR organic and rBC mass  
236 spectral and PToF signals with the ADIc. The SP-AMS measurements were conducted by  
237 switching the laser on and off. Laser off data was utilized when the SP-AMS was compared with  
238 the ACSM+ADIc and laser on data was used for the period when the ADIc was installed in front  
239 of the SP-AMS. The default CE of 0.5 for ambient particles was applied to both ACSM and SP-  
240 AMS data. An RH sensor was installed in the ACSM line after the ADIc. Ambient meteorological  
241 parameters were recorded at the Kumpula Weather station. Field measurements at SMEAR III  
242 were conducted between 13 July to 22 October 2018, with sampling on about 27 different days.  
243 Temperature settings of the ADIc during the field campaigns at ARI and FMI are given in Table  
244 1.



## 245 **3 Results and discussion**

### 246 **3.1 Laboratory evaluation**

#### 247 **3.1.1 Concentration factor**

248 Figure 2 shows laboratory results for monodisperse AS particles for two flow regimes. The  
249 measured concentration factor, defined as the ratio of particle number concentration in the output  
250 flow of the ADIc to that in the sample flow, is plotted as a function of particle mobility diameter.  
251 Data for the lower flow regime is from Prototype 1, which was subsequently tested at ARI for  
252 aerosol chemical species. For the lower flow, the average measured CF was  $7.7 \pm 0.3$  for the  
253 particles larger than 15 nm, compared to a theoretical CF of 8.3. Data shown for the higher flow  
254 regime was obtained with Prototype 2, which was later tested at FMI for particle chemistry and  
255 size distributions. For the higher flow, the measured CF was  $11.9 \pm 0.2$ , compared to a theoretical  
256 CF of 13.6, for 50–305 nm particles. When operated in the lower flow regime, Prototype 2 data is  
257 similar to that for Prototype 1, with a measured CF of  $7.0 \pm 0.5$  (data not shown). The influence of  
258 ADIc on particle size was investigated in more detail with aerosol mass spectrometers (Sect.  
259 3.1.2.).

260 The ratio of measured to theoretical CF was  $\sim 0.9$  (see Table 2), suggesting that 90 % of the  
261 particles in the sample flow were focused into the output concentrated flow. In the experiments  
262 conducted on Prototype 1, the particle concentration was also measured in the discard flow, and it  
263 accounted for  $9 \pm 2$  % of the sampled particle concentration at sizes above 20 nm, on average. The  
264 fraction of particles in the discard flow showed a small, but systematic, dependence on particle  
265 size with the fraction decreasing from 12 % at 18 nm to 6 % at 600 nm. The unaccounted particles  
266 (2 % on average) were presumably lost in the transport lines or in the focusing nozzle itself.

267 To evaluate the stability of the ADIc, both prototypes were operated for several days while  
268 sampling laboratory air. Particle number concentrations were measured in the sample flow and in  
269 the output flow. Particle concentration varied between 900 and 15000 # cm<sup>-3</sup>. For the lower flow  
270 regime data (Fig. S2a–b), the measured CF was of  $5.7 \pm 0.4$  with the theoretical CF of 7.5. Linear  
271 regression of that data yielded a correlation coefficient ( $R^2$ ) of 0.984. In the higher flow regime  
272 (Fig. S2c–d), the measured CF was  $9.0 \pm 0.7$ , with a theoretical CF of 13.6. For that data the  
273 correlation coefficient ( $R^2$ ) was 0.940. It is important to note that particle concentrations were



274 measured using CPCs with a 5 nm activation threshold while the ADIC threshold is closer to 10  
275 nm. Thus, particles below 10 nm in the ambient size distribution would not be concentrated,  
276 leading to a lower measured CF and a lower ratio of measured/theoretical CF than in Table 2. In  
277 addition, changes in the ambient size distribution can lead to some variability in the measured CF.  
278 Importantly, no systematic change was observed throughout the experiments.

279

### 280 3.1.2 Chemical composition and particle size

281 The dependence of CF on particle chemical composition was evaluated in the laboratory with size-  
282 selected 300 nm AS and AN particles and a subsequent analysis of concentrated aerosol by an HR-  
283 AMS. The theoretical and the measured CF for ammonium and sulfate from AS and for ammonium  
284 and nitrate from AN are given in Table 2. Compared to CF obtained for particle number  
285 concentration, the ratio of measured to theoretical CF was the same for AS while for AN the  
286 measured CF was slightly closer to the theoretical CF.

287 The influence of the ADIC on particle size was investigated by using monodisperse AS, AN and  
288 DOS particles in the size range of 30 to 340 nm (mobility diameter). Size and chemical  
289 composition of particles with and without the ADIC were analyzed by an SP-AMS. Measurements  
290 were carried out in the high flow regime (theoretical CF of 21.3). Figure 3 shows the vacuum  
291 aerodynamic diameter ( $d_{va}$ ) for sulfate (from AS), nitrate (from AN) and organics (from DOS) as  
292 measured for concentrated versus unconcentrated aerosol. The regression slope was 1.02, the  
293 intercept was -2.51, and the correlation coefficient ( $R^2$ ) was 0.999 showing that the particle  
294 diameter was not changed by passing through the ADIC for any of the measured particle sizes or  
295 chemical species.

296

## 297 3.2 Field Evaluation

### 298 3.2.1 Ambient organics and rBC

299 The performance of the ADIC for ambient aerosol was examined at two locations; at a roof top  
300 sampling station on the ARI building and at SMEAR III in Helsinki. In order to investigate the  
301 impact of the ADIC on aerosol organic and rBC chemistry, the SP-AMS was installed behind the



302 ADIc at SMEAR III and measured alternately from the output flow of the ADIc and a bypass line.  
303 Measurements were performed on 11 different days in June, July and August 2018 with a total  
304 sampling time of ~7 hours behind the ADIc and ~7 hours in bypass. Average high-resolution mass  
305 spectra for organics and rBC with and without the ADIc are presented in Fig. 4. In general, organics  
306 at SMEAR III were highly oxygenated with large oxygen to carbon ratio (O:C) and large organic  
307 carbon to organic matter ratio (OC:OM). The elemental composition of organics did not change  
308 noticeably when the sample was passed through the ADIc. The correlation between the mass  
309 spectral ions with and without the ADIc for each fragment family are presented in Fig. 4 c–f. The  
310 correlation was uniformly high ( $R^2 > 0.987$ ) and the slope describing the measured CF was on  
311 average  $19.2 \pm 3.2$ . The slope was smallest for the most oxygenated fragment family  $C_xH_yO_z, z>1$   
312 and largest for  $C_x$  (rBC) and was smaller than theoretical CF (21.3) for all families except the  $C_x$   
313 family. Smaller measured than theoretical CF is in agreement with the results obtained in the  
314 laboratory tests (see Table 2) while the reason for a larger measured than theoretical CF for  $C_x$  is  
315 still unclear. Overall, based on these tests, it can be concluded that passing through the ADIc does  
316 not significantly change the fragmentation or the elemental composition of organics in the ambient  
317 particles.

318

### 319 3.2.2 Mass size distributions

320 The SP-AMS data with and without the ADIc was also used to investigate the impact of the ADIc  
321 on particle mass size distributions. Figure 5 compares the mass size distribution for organics,  
322 sulfate, nitrate and ammonium sampling through the ADIc and sampling from the bypass line. The  
323 PToF data was collected and analyzed in unit mass resolution (UMR) mode. Figure 5 demonstrates  
324 that the size distribution of ambient aerosol particles was not affected by passing through the ADIc.  
325 In addition, Fig. 5d shows significant improvement in signal to noise for ammonium when  
326 concentrating the sample flow.

327 Additional SP-AMS size distribution data was collected and analyzed in HR mode on one day with  
328 a total sampling time of 70 minutes in bypass and 70 minutes through the ADIc. HR size  
329 distributions are shown in Fig. 6 for major chemical species and for several specific fragment ions.  
330 The much higher signal to noise in the concentrated PToF traces gives better chemical resolution  
331 of the size distribution. The bimodal size distribution for organics is clear in the ADIc data in Fig.



332 6a with hydrocarbon-like fragments (e.g., C<sub>3</sub>H<sub>7</sub> and C<sub>4</sub>H<sub>9</sub> in Fig. 6h and 6k) contributing to the  
333 mode at  $d_{va} = 160$  nm and more oxygenated fragments (e.g., C<sub>2</sub>H<sub>3</sub>O, CO<sub>2</sub>, C<sub>2</sub>H<sub>4</sub>O<sub>2</sub> and C<sub>3</sub>H<sub>5</sub>O in  
334 Fig. 6g, 6i, 6j and 6l) contributing to the mode at  $d_{va} = 400$  nm. In addition, the higher signal to  
335 noise in the concentrated sample enables PToF measurement for very small signals such as  
336 chloride (Fig. 6e) or CO<sub>2</sub> (Fig. 6i) and improves the PToF measurement for smaller signals such  
337 as rBC (Fig. 6f).

338

### 339 3.2.3 Long-term Stability

340 The long-term operation of the ADIc was tested at ARI where it ran for more than three weeks  
341 without user maintenance or intervention. The measured CFs from comparing the Q-AMS mass  
342 loading to the HR-AMS mass loading are presented in Fig. 7 with the average values presented in  
343 Table 3. The theoretical CF was calculated from the ADIc discard flow rate and the Q-AMS inlet  
344 flow rate (equal to ADIc outlet flow) as theoretical CF = (discard flow + Q-AMS inlet flow)/Q-  
345 AMS inlet flow. Discard and Q-AMS flows were logged in real-time. The slight variation in  
346 theoretical CF was due to variations in the Q-AMS inlet flow rate, not variations in the discard  
347 flow. The gap in the data between 21 and 23 August 2014 was due to an issue with the HR-AMS,  
348 not with the ADIc.

349 The measured CFs for nitrate and sulfate were 85 to 90 % of theoretical CFs, consistent with the  
350 laboratory measurements presented in Table 2. The measured CF for ammonium was higher than  
351 the theoretical value which may indicate that the aqueous droplets in the ADIc initiator and  
352 moderator stages absorbed gas-phase ammonia that remained in the particles after drying. This  
353 effect has been observed for acidic particles in the miniature VACES (Saarikoski et al., 2014). The  
354 ambient aerosol in this study was possibly slightly acidic with an average ratio of measured to  
355 predicted ammonia of  $0.9 \pm 0.15$  in the HR-AMS data. Another possibility is that the RIE for  
356 ammonium was incorrect for one or both of the instruments, even though it was measured three  
357 times during the experiment. This is supported by the fact that the measured CF was greater than  
358 one during periods when the Q-AMS was bypassing the ADIc (Table 3).

359 The measured concentration factor ( $6.1 \pm 0.8$ ) for organics was much lower than the theoretical  
360 value ( $10.5 \pm 0.3$ ). This was caused by a difference in the cutoff of the aerodynamic lenses in the



361 two AMS instruments. During this time period, organics were dominated by emissions from road  
362 paving activities which generate large, hydrocarbon-like particles. Figure S3 shows the size  
363 distributions for organics, mass-to-charge ratio ( $m/z$ ) 44 and  $m/z$  57 for the HR-AMS and the Q-  
364 AMS+ADIC. It is clear that the size distributions for organics and  $m/z$  57 from the Q-AMS were  
365 missing mass above  $d_{va} \sim 700$  nm that was measured by the HR-AMS, leading to a lower measured  
366 CF for organics. The  $m/z$  44 size distributions, representative of accumulation mode aerosol  
367 particles, were similar in the two instruments because the mass of  $m/z$  44 was below the lens cutoff.  
368 The measured CF for  $m/z$  44 in Fig. S3b was 9.2 while the measured CF for  $m/z$  57 in Fig. S3c  
369 was only 3.9. The measured CF for organics also showed a larger diurnal variation than the  
370 measured CFs for the other species (Fig. 7), likely because road paving activities took place at  
371 night leading to a lower measured CF at night-time.

372

### 373 3.2.4 Concentrating under high and low flow regimes

374 The performance of the ADIC with ambient aerosol was also tested systematically under two flow  
375 regimes. Although the growth tube in the ADIC is sized for low-flow operation, in some cases it  
376 can be beneficial to operate the ADIC with the largest possible CF, for example, when very small  
377 signals (e.g., metals, PToF) are of interest, or the ambient concentrations are extremely low. High  
378 ( $1.7 \text{ L min}^{-1}$ ) and low ( $1.0 \text{ L min}^{-1}$ ) sample flows, resulting in theoretical CFs of 21.3 and 12.5,  
379 respectively, were investigated at SMEAR III with the ADIC installed in front of an ACSM while  
380 the SP-AMS was sampling from the bypass line. The data from the ACSM+ADIC was corrected  
381 for the CF by dividing the concentrations by  $0.9 \cdot$  theoretical CF since the laboratory tests and the  
382 field campaign at ARI suggest that the measured CF is likely to be 90 % of the theoretical CF.

383 The time series of all chemical species measured with the ACSM+ADIC and SP-AMS track each  
384 other well and the average mass loadings agreed within 20–30 % (Fig. 8), within the estimated  
385 uncertainty of 34–38 % for AMS measurements (Bahreini et al., 2009). In the high flow regime,  
386 the corrected ACSM+ADIC mass loadings were systematically higher for organics, sulfate and  
387 ammonium compared to the SP-AMS. This might be caused by the lack of simultaneous  
388 measurement of the sample flow rate, so that any error in the sample flow rate before/after the  
389 experiment could propagate into the theoretical CF and thus into the correction factor. For nitrate,  
390 the corrected ACSM+ADIC mass loading varied above the SP-AMS during the afternoon and



391 below during the night. Under low flow conditions, there was a time period of about 12 hours on  
392 18 and 19 September when the corrected ACSM+ADIC mass loadings for nitrate and chloride were  
393 much lower than corresponding mass loadings from the SP-AMS. During this period, the aerosol  
394 particles were also not neutralized (i.e., measured ammonium was lower than ammonium predicted  
395 from the measured anions). Based on the ratio of  $m/z$  46 to  $m/z$  30, nitrate was in the form of  
396 inorganic nitrate (e.g.,  $\text{NH}_4\text{NO}_3$ ) rather than organic nitrates. The reason for the lower  
397 concentrations of nitrate and chloride with the ACSM+ADIC during this 12 hour period is not  
398 clear.

399 The relative humidity was measured after the ADIC near the Q-ACSM inlet. RH was relatively  
400 constant at  $63 \pm 6$  %, consistent with a dewpoint of  $16$  °C at the outlet of the ADIC and a room  
401 temperature of about  $25$  °C. This was somewhat higher than the recommended operating RH of  
402 20–40 % for AMS/ACSM instruments, but not high enough to cause an increase in the collection  
403 efficiency (Middlebrook et al., 2012). However, using a dryer in between the ADIC and the  
404 AMS/ACSM would reduce any potential uncertainty due to RH affecting CE.

405 In terms of Q-ACSM measurement, a particularly important improvement in signal to noise with  
406 the ADIC was achieved. Figs. 9a and 9b show 30-minute time resolution data collected with the  
407 Q-ACSM without the ADIC, and Figs. 9b and 9d display 10-minute time resolution data collected  
408 with the Q-ACSM+ADIC for ammonium and  $m/z$  60, a tracer  $m/z$  for biomass burning. Compared  
409 to the SP-AMS data averaged to the same time resolution, it is evident that the signal to noise for  
410 the concentrated Q-ACSM data is similar to the SP-AMS. As a consequence, use of the ADIC with  
411 the ACSM will improve determination of ammonium and thus provide better estimates of particle  
412 neutralization and CE for ambient aerosol. In addition, better signal to noise for tracer  $m/z$ 's will  
413 improve source apportionment with statistical methods such as positive matrix factorization  
414 (PMF).

415

#### 416 **4 Conclusions**

417 The ADIC is tailored for the low ( $\sim 0.08$  L  $\text{min}^{-1}$ ) inlet flow of aerosol mass spectrometers such as  
418 the AMS and ACSM and provides a factor of 8–21 enrichment in the concentration of particles.  
419 This concentration factor depends primarily on the ratio between the sample flow and the output



420 flow, and is found to be independent of particle size above about 10 nm. The system is relatively  
421 small, and easily interfaced with the AMS.

422 Particle chemical composition and particle size measured with an SP-AMS were not affected by  
423 the condensational growth and evaporation process in the ADIc. Moreover, the ADIc ran  
424 unattended for a period of almost one month at a field site. Measured concentration factors for  
425 ambient aerosol particles in two different locations showed some variation that is not fully  
426 understood. However, the ADIc provides improved detection of low signals that outweighs a slight  
427 increase in uncertainty in the mass loadings. Improved detection limits will be important especially  
428 in remote areas where particle concentrations are low, and for measuring size distributions that  
429 typically need longer averaging periods. Additionally, use of the ADIc will be important for  
430 improving source apportionment with Q-ACSM data by gaining better time-resolution and/or  
431 signal to noise ratio.

432

433 *Data availability.* Data presented in this article is available upon request.

434

435 *Supplement.* The supplement related to this article is available online

436

437 *Competing interests.* Aerosol Dynamics Inc. holds a patent on the particle focusing technology.

438

439 *Author contributions.* SS, HT, SVH, AEF and LRW designed the experiments. MA, KT, LRW,  
440 PC, TH, AEF, SRS, and GSL conducted measurements in laboratory and field. Data analysis and  
441 interpretation of the measurement data was done by SS, LRW, AEF and SVH. Working  
442 environment and financial support was provided by HT at FMI, JTJ and DRW at Aerodyne and  
443 SVH at Aerosol Dynamics. SS, LRW and SVH prepared the manuscript with contributions from  
444 all co-authors.

445

446 *Acknowledgements.* Funding is gratefully acknowledged from the US Department of Energy,  
447 Small Business Research Program (grant # DESC0004698), the Cityzer (Business Finland project





448 Dnro:3021/31/2015), TAQIITA (Business Finland project Dnro:2634/31/2015) and the Launching  
449 Regional Innovations and Experimentations Funds (AIKO), governed by the Helsinki Regional  
450 Council (project HAQT, AIKO014).

451

452

#### 453 **References**

454 Asmi, E., Frey, A., Virkkula, A., Ehn, M., Manninen, H. E., Timonen, H., Tolonen-Kivimäki, O.,  
455 Aurela, M., Hillamo, R., and Kulmala, M.: Hygroscopicity and chemical composition of Antarctic  
456 sub-micrometre aerosol particles and observations of new particle formation, *Atmos. Chem. Phys.*,  
457 10, 4253–4271, 2010.

458 Bahreini, R., Ervens, B., Middlebrook, A., Warneke, C., De Gouw, J., DeCarlo, P., Jimenez, J.,  
459 Brock, C., Neuman, J., Ryerson, T., Stark, H., Atlas, E., Brioude, J., Fried, A., Holloway, J. S.,  
460 Peischl, J., Richter, D., Walega, J., Weibring, P., Wollny, A. G., and Fehsenfeld, F. C.: Organic  
461 aerosol formation in urban and industrial plumes near Houston and Dallas, Texas, *J. Geophys. Res.*  
462 114, <https://doi.org/10.1029/2008JD011493>, 2009.

463 Budisulistiorini, S., Canagaratna, M., Croteau, P., Baumann, K., Edgerton, E., Kollman, M., Ng,  
464 N., Verma, V., Shaw, S., and Knipping, E.: Intercomparison of an Aerosol Chemical Speciation  
465 Monitor (ACSM) with ambient fine aerosol measurements in downtown Atlanta, Georgia, *Atmos.*  
466 *Meas. Tech.*, 7, 1929–1941, 2014.

467 Canagaratna, M. R., Jayne, J. T., Jimenez, J. L., Allan, J. D., Alfarra, M. R., Zhang, Q., Onasch,  
468 T. B., Drewnick, F., Coe, H., Middlebrook, A., Delia, A., Williams, L. R., Trimborn, A. M.,  
469 Northway, M. J., DeCarlo, P. F., Kolb, C. E., Davidovits, P., and Worsnop, D. R.: Chemical and  
470 Microphysical Characterization of Ambient Aerosols with the Aerodyne Aerosol Mass  
471 Spectrometer, *Mass Spectrom. Rev.*, 26, 185–222, 2007.

472 Carbone, S., Onasch, T., Saarikoski, S., Timonen, H., Saarnio, K., Sueper, D., Rönkkö, T., Pirjola,  
473 L., Häyrynen, A., Worsnop, D., and Hillamo, R.: Characterization of trace metals on soot particles  
474 with the SP-AMS: detection and quantification, *Atmos. Meas. Tech.*, 8, 4803–4815, 2015.

475 DeCarlo, P. F., Kimmel, J. R., Trimborn, A., Northway, M. J., Jayne, J. T., Aiken, A. C., Gonin,  
476 M., Fuhrer, K., Horvath, T., Docherty, K. S., Worsnop, D. R., and Jimenez, J. L.: Field-deployable,  
477 high-resolution, time-of-flight aerosol mass spectrometer, *Anal. Chem.*, 78, 8281–8289,  
478 doi:10.1021/ac061249n, 2006.

479 Eiguren Fernandez, A., Lewis, G. S., and Hering, S. V.: Design and Laboratory Evaluation of a  
480 Sequential Spot Sampler for Time-Resolved Measurement of Airborne Particle Composition,  
481 *Aerosol Sci. Technol.*, 48, 655–663, 2014.

482 Fuerstenau, S., Gomez, A., and J. Fernandez de la Mora, J.: Visualization of aerodynamically  
483 focused subsonic aerosol jets, *J. Aerosol Sci.*, 25, 165–173, 1994.



484

485 Geller, G. D., Biswas, S., Fine, P. M., and Sioutas, C.: A new compact aerosol concentrator for  
486 use in conjunction with low flow-rate continuous aerosol instrumentation, *J. Aerosol Sci.*, 36,  
487 1006–1022, 2005.

488 Gupta, T., Demokritou, P., and Koutrakis, P.: Development and Performance Evaluation of a High  
489 Volume Ultrafine Particle Concentrator for Inhalation Toxicological Studies, *Inhal. Toxicol.*, 16,  
490 1–12, 2004.

491 Hering, S.V., Spielman, S.R., and Lewis, G.S.: Moderated, water-based, condensational particle  
492 growth in a laminar flow, *Aerosol Sci. Technol.*, 48, 401–408, 2014.

493 Hering, S.V., Lewis, G.S., Spielman, S.R., and Eiguren-Fernandez, A.: A MAGIC Concept for  
494 Self-Sustained, Water based, Ultrafine Particle Counting, *Aerosol Sci. Technol.*, 53, 63-72, 2018.

495 IPCC: Climate Change Synthesis Report. Contribution of Working Groups I, II and III to the Fifth  
496 Assessment Report of the Intergovernmental Panel on Climate Change [Core Writing Team, R.K.  
497 Pachauri and L.A. Meyer (eds.)]. IPCC, Geneva, Switzerland, 151 pp. 2014. 2014.

498 Jung, H., Arellanes, C., Zhao, Y., Paulson, S., Anastasio, C., and Wexler, A.: Impact of the  
499 Versatile Aerosol Concentration Enrichment System (VACES) on Gas Phase Species, *Aerosol  
500 Sci. Technol.*, 44, 1113–1121, 2010.

501 Järvi, L., Hannuniemi, H., Hussein, T., Junninen, H., Aalto, P. P., Hillamo, R., Mäkelä, T.,  
502 Keronen, P., Siivola, E., Vesala, T., and Kulmala, M.: The urban measurement station SMEAR  
503 III: Continuous monitoring of air pollution and surface-atmosphere interactions in Helsinki,  
504 Finland, *Boreal Environ Res*, 14, 86–109, 2009.

505 Khlystov, A., Zhang, Q., Jimenez, J. L., Stanier, C., Pandis, S. N., Canagaratna, M. R., Fine, P.,  
506 Misra, C., and Sioutas, C.: In situ concentration of semi-volatile aerosol using water-condensation  
507 technology, *J. Aerosol Sci.*, 36, 866–880, 2005.

508 Kim, S., Jaques, P. A., Chang, M. C., Barone, T., Xiong, C., Friedlander, S. K., and Sioutas, C.:  
509 Versatile aerosol concentration enrichment system (VACES) for simultaneous in vivo and in vitro  
510 evaluation of toxic effects of ultrafine, fine and coarse ambient particles – Part II: field evaluation,  
511 *J. Aerosol Sci.*, 32, 1299–1314, 2001.

512 Kreisberg, N.M., Spielman, S.R., Eiguren-Fernandez, A., Hering, S.V., Lawler, M.J., Draper,  
513 D.C., and Smith, J.N.: Water condensation-based nanoparticle charging system: Physical and  
514 chemical characterization, *Aerosol Sci. Technol.*, 52, 1167–1177, 2018.

515 Lelieveld, J., Evans, J. S., Fnais, M., Giannadaki, D., and Pozzer, A.: The contribution of outdoor  
516 air pollution sources to premature mortality on a global scale, *Nature*, 525, 367–371, 2015.

517 Liu, P. S. K., Deng, R., Smith, K. A., Jayne, J. T., Williams, L. R., Canagaratna, M. R., Moore,  
518 K., Onasch, T. B., Worsnop, D. R., and Deshler, T.: Transmission Efficiency of an Aerodynamic



- 519 Focusing Lens System: Comparison of Model Calculations and Laboratory Measurements for the  
520 Aerodyne Aerosol Mass Spectrometer, *Aerosol Sci. Technol.*, 41, 721–733, 2007.
- 521 Middlebrook, A. M., Bahreini, R., Jiménez, J. L., and Canagaratna, M. R.: Evaluation of  
522 composition-dependent collection efficiencies for the Aerodyne aerosol mass spectrometer using  
523 field data, *Aerosol Sci. Technol.* 46, 258–271, 2012.
- 524 Ng, N. L., Herndon, S. C., Trimborn, A., Canagaratna, M. R., Croteau, P. L., Onasch, T. B.,  
525 Sueper, D., Worsnop, D. R., Zhang, Q., Sun, Y. L., and Jayne, J. T.: An Aerosol Chemical  
526 Speciation Monitor (ACSM) for Routine Monitoring of the Composition and Mass Concentrations  
527 of Ambient Aerosol, *Aerosol Sci. Technol.*, 45, 780–794, 2011.
- 528 Onasch, T. B., Trimborn, A., Fortner, E. C., Jayne, J. T., Kok, G. L., Williams, L. R., Davidovits,  
529 P., and Worsnop, D. R.: Soot Particle Aerosol Mass Spectrometer: Development, Validation, and  
530 Initial Application, *Aerosol Sci. Technol.*, 46, 804–817, 2012.
- 531 Pan, M., Eiguren-Fernandez, A., Hsieh, H., Afshar-Mohajer, N., Hering, S. V., Lednický, J., Hung  
532 Fan, Z., and Wu, C. Y.: Efficient collection of viable virus aerosol through laminar-flow, water-  
533 based condensational particle growth, *J Appl. Microbiol.*, 120, 805–815, 2016.
- 534 Pope, C. A., and Dockery, D.W.: Health Effects of Fine Particulate Air Pollution: Lines that  
535 Connect, *J. Air & Waste Manage. Assoc.*, 56, 709–742, 2006.
- 536 Saarikoski, S., Carbone, S., Cubison, M. J., Hillamo, R., Keronen, P., Sioutas, C., Worsnop, D. R.,  
537 and Jimenez, J. L.: Evaluation of the performance of a particle concentrator for online  
538 instrumentation, *Atmos. Meas. Tech.*, 7, 2121–2135, 10.5194/amt-7-2121-2014, 2014.
- 539 Stolzenburg, M, N. Kreisberg, and S. Hering.: Atmospheric size distributions measured by  
540 differential mobility optical particle size spectrometry, *Aerosol Sci. Technol.*, 29, 402–418, 1998.
- 541 Tunved, P., Hansson, H. C., Kerminen, V. M., Strom, J., Maso, M. D., Lihavainen, H., Viisanen,  
542 Y., Aalto, P. P., Komppula, M., and Kulmala, M.: High natural aerosol loading over boreal forests,  
543 *Science*, 312, 261–263, 2006.
- 544 Zauscher, M. D., Moore, M. J., Lewis, G. S., Hering, S. V., and Prather, K. A.: Approach for  
545 measuring the chemistry of individual particles in the size range critical for cloud formation, *Anal.*  
546 *Chem.*, 83, 2271–2278, 2011.
- 547
- 548



**Table 1.** Approximate temperature and flow settings for the ADIC experiments presented in this study. ADI = Aerosol Dynamics Inc., ARI = Aerodyne Research, Inc., FMI = Finnish Meteorological Institute. Tcon, Tini, Tmod and Tnoz are the operating temperatures for the conditioner, initiator, moderator and focusing nozzle, respectively. AN, AS, DOS are abbreviations for ammonium nitrate, ammonium sulfate and dioctyl sebacate, respectively.

Test site	ADI	ADI	ADI	ARI	ARI	FMI	FMI	FMI
<b>Prototype No.</b>	1	2	2	1	1	2	2	2
<b>Test type</b>	Lab	Lab	Lab	Lab	Field	Lab	Field	Field
<b>Measured parameters/ species</b>	Particle number and size	Particle number	Particle number and size	AN, AS	Chemical composition and size	AN, AS, DOS and particle size	Chemical composition	Chemical composition, size
<b>Tcond ( °C)</b>	5	5	6	5	5	6	10	10
<b>Tinit ( °C)</b>	26	26	31	26	26	31	31	31
<b>Tmod ( °C)</b>	10	10	8	10	10	8	13	13
<b>Tnoz( °C)</b>	30	30	35	30	30	35	35	35
<b>Tout ( °C)</b>	35	35	35	n/a	n/a	35	35	35
<b>Sample Flow (L min<sup>-1</sup>)</b>	1.0	1.0	1.5	0.9	0.9	1.7	1.0	1.7
<b>Output Flow (L min<sup>-1</sup>)</b>	0.12	0.11	0.11	0.08	0.08	0.08	0.08	0.08
<b>Theoretical CF</b>	8.3	9.1	13.6	11.3 <sup>a</sup> / 12.6 <sup>b</sup>	11.3	21.3	12.5	21.3

<sup>a</sup> AN, <sup>b</sup> AS



**Table 2.** Measured and theoretical concentration factors (CFs) for ammonium nitrate (AN) and ammonium sulfate (AS) obtained in the laboratory tests.

Material	Measured species	Measured CF	Theoretical CF	Measured/ Theoretical CF
AS	Particle number	7.4	8.3	0.89
	Particle number	11.9	13.6	0.88
	Ammonium	11.2	12.6	0.89
	Sulfate	11.3	12.6	0.89
AN	Ammonium	10.6	11.3	0.94
	Nitrate	10.6	11.3	0.94

560

**Table 3.** Measured and theoretical concentration factors, and average mass loadings in ambient measurements at ARI. The measured CF was calculated from the ratio of Q-AMS+ADiC to HR-AMS mass loadings. In the bypass line the sample was not concentrated. The theoretical CF was calculated from the ADiC discard flow rate and the Q-AMS inlet flow rate (see text for details).

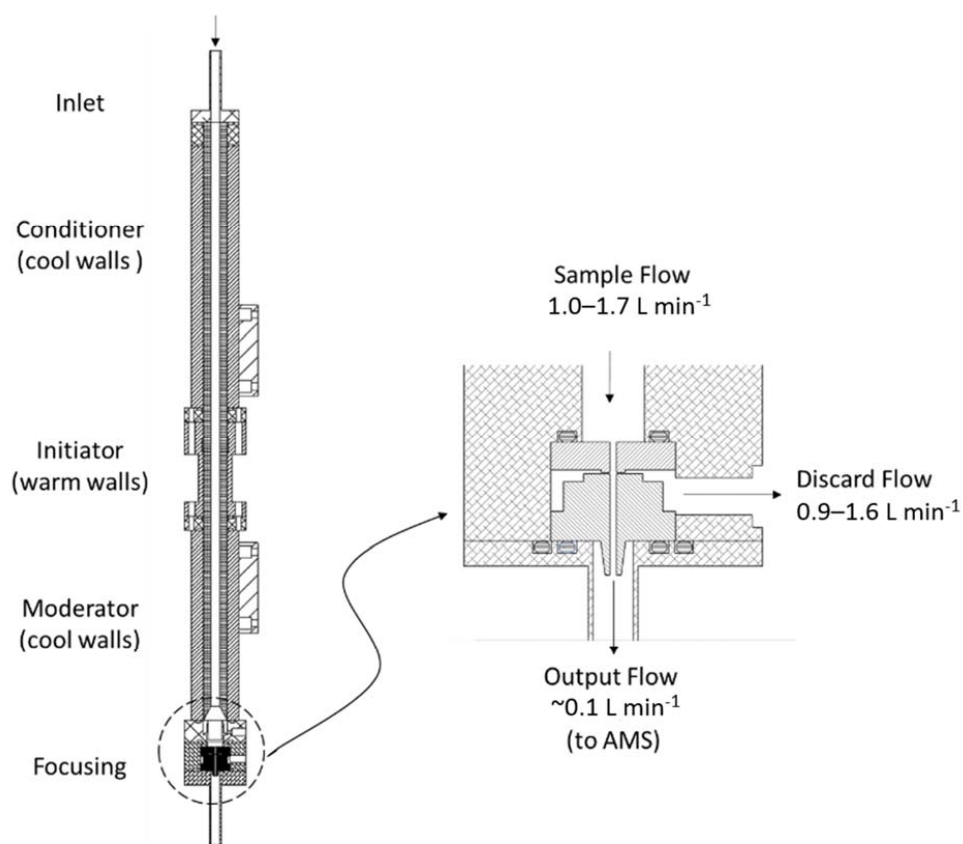
565

		Through ADiC	Bypass
Measured CF	Organics	$6.1 \pm 0.8$	$0.7 \pm 0.06$
	Sulfate	$9.7 \pm 1.5$	$1.0 \pm 0.1$
	Nitrate	$9.1 \pm 1.1$	$1.0 \pm 0.1$
	Ammonium	$12.7 \pm 1.9$	$1.3 \pm 0.4$
Theoretical CF		$10.5 \pm 0.3$	1.0

570

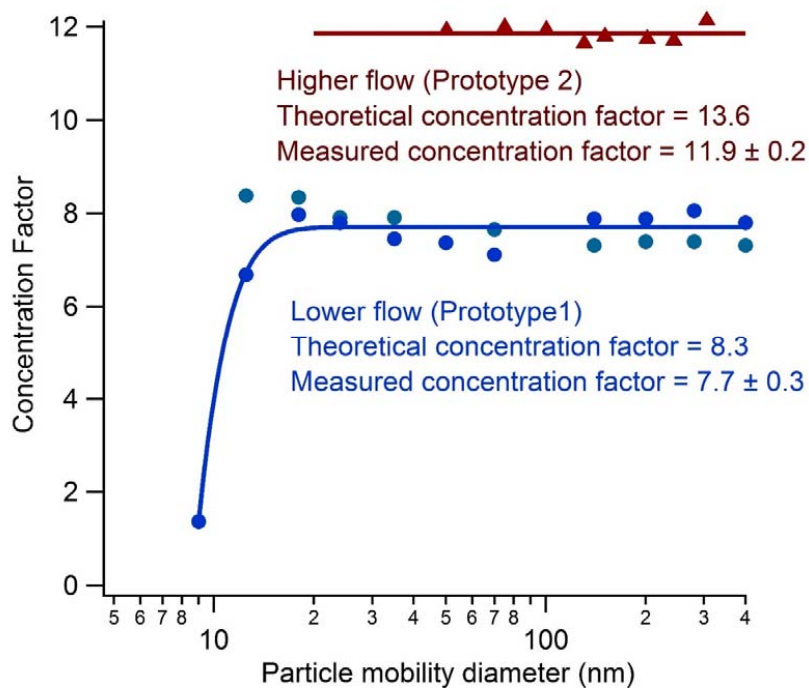


Figures



575

**Figure 1.** Schematic of the Aerosol Dynamics Inc. concentrator (ADIC) with enlargement of the focusing nozzle.



580

**Figure 2.** Size dependent concentration factor for the ADIc for higher (triangles) and lower (circles) flow regimes as a function of particle size. The red line indicates the average of the higher flow data. The blue line is a guide for the eye. Data are from two different prototype instruments, as indicated.

585

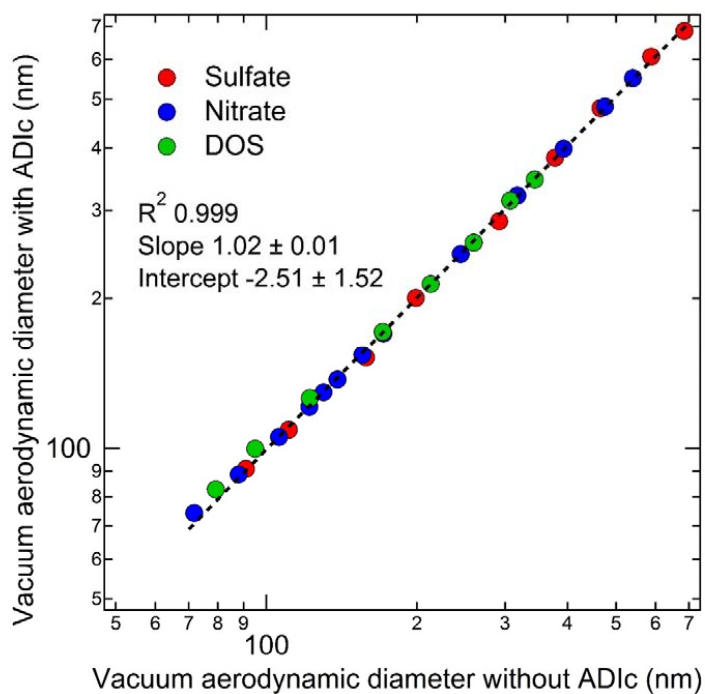


**Figure 3.** Particle size measured with an SP-AMS for 70–700 nm particles (vacuum aerodynamic diameter) of sulfate, nitrate and organics (from DOS) with and without concentration by the ADIc.  
590 Corresponding mobility diameters were 30–340 nm.



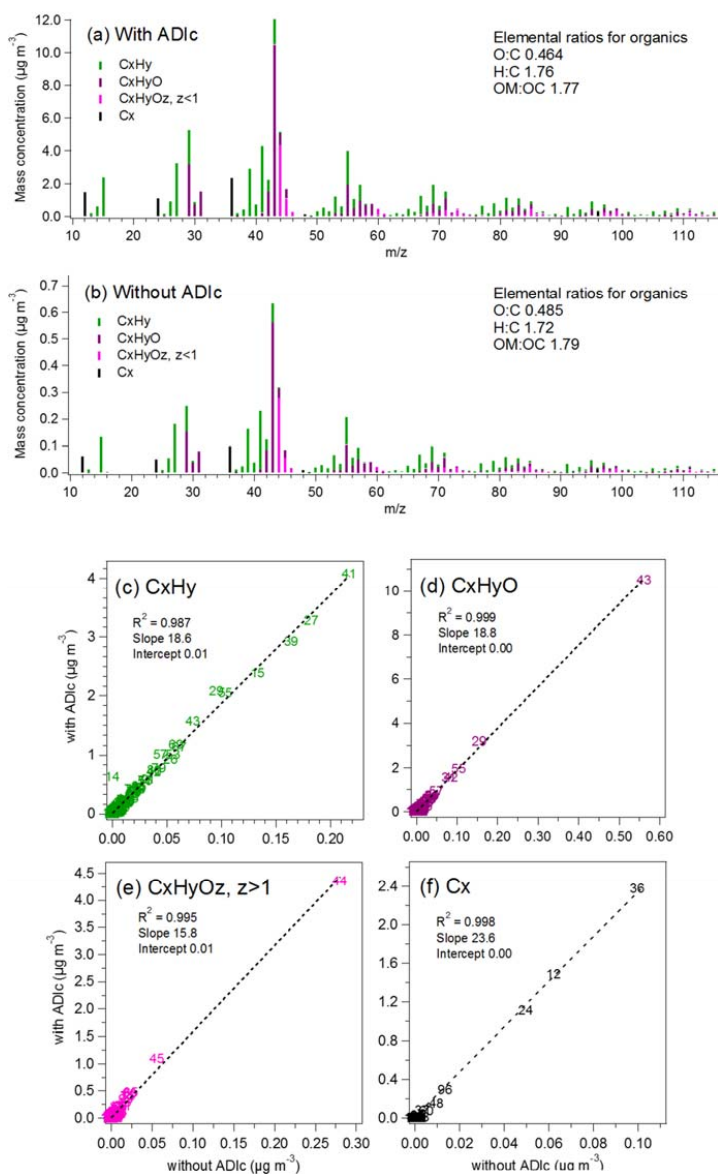


**Figure 4.** Mass spectra for ambient organics and rBC measured with and without ADIc (a–b) and the correlation of AMS fragment families (c–f) at SMEAR III, Helsinki. Theoretical concentration

595 factor was 21.3.

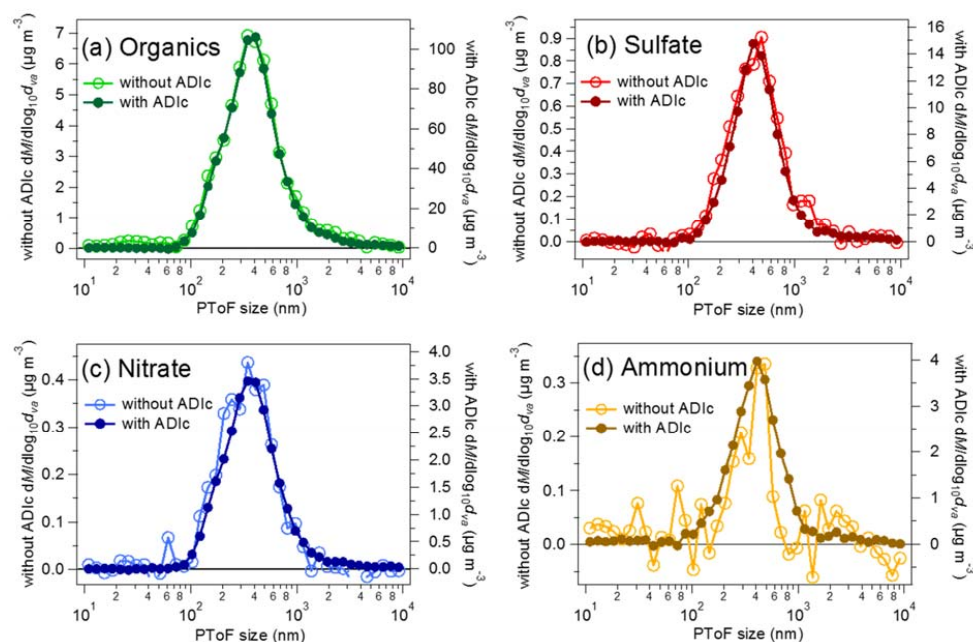
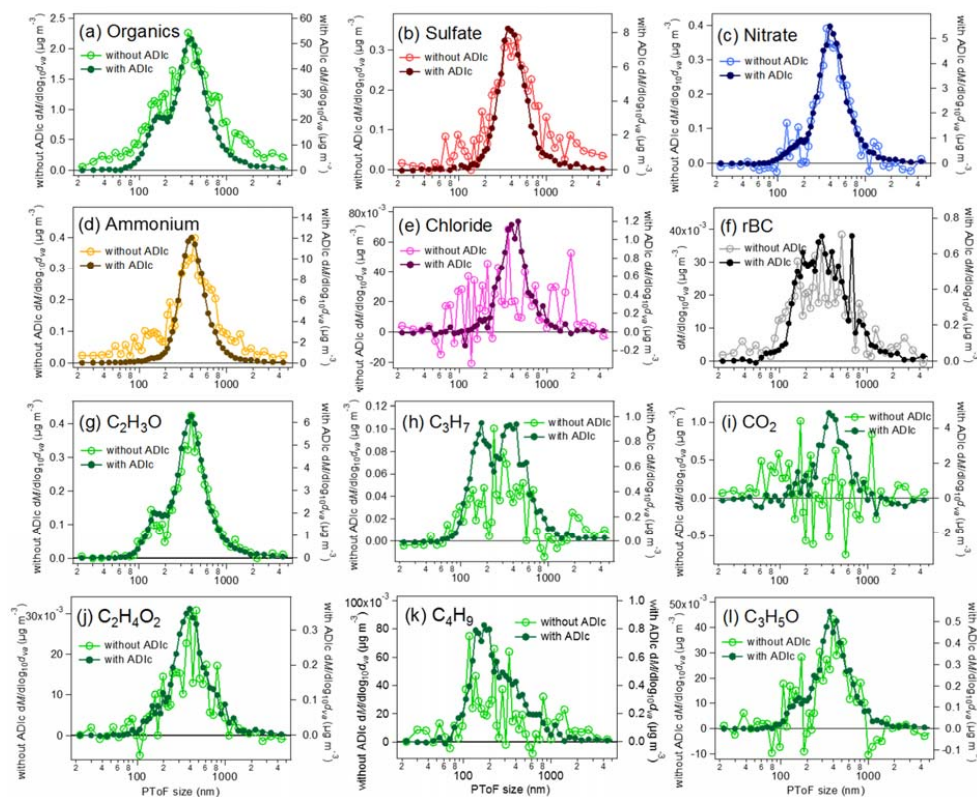


**Figure 5.** Mass size distributions measured without (left axis) and with (right axis) the ADic for organics (a), sulfate (b), nitrate (c) and ammonium (d) in UMR mode at SMEAR III. Sampling time for each size distribution was 70 minutes with the ADic and 70 minutes without the ADic. The theoretical concentration factor was 21.3.



605

**Figure 6.** Mass size distributions measured without (left axis) and with the ADic (right axis) for organics (a), sulfate (b), nitrate (c), ammonium (d), chloride (e), rBC (f), C<sub>2</sub>H<sub>3</sub>O (g), C<sub>3</sub>H<sub>7</sub> (h), CO<sub>2</sub> (i), C<sub>2</sub>H<sub>4</sub>O<sub>2</sub> (j), C<sub>4</sub>H<sub>9</sub> (k) and C<sub>3</sub>H<sub>5</sub>O (l) in HR mode at SMEAR III. Sampling time for each size distribution was 70 minutes without and 70 minutes with the ADic. Theoretical concentration factor was 21.3.

610

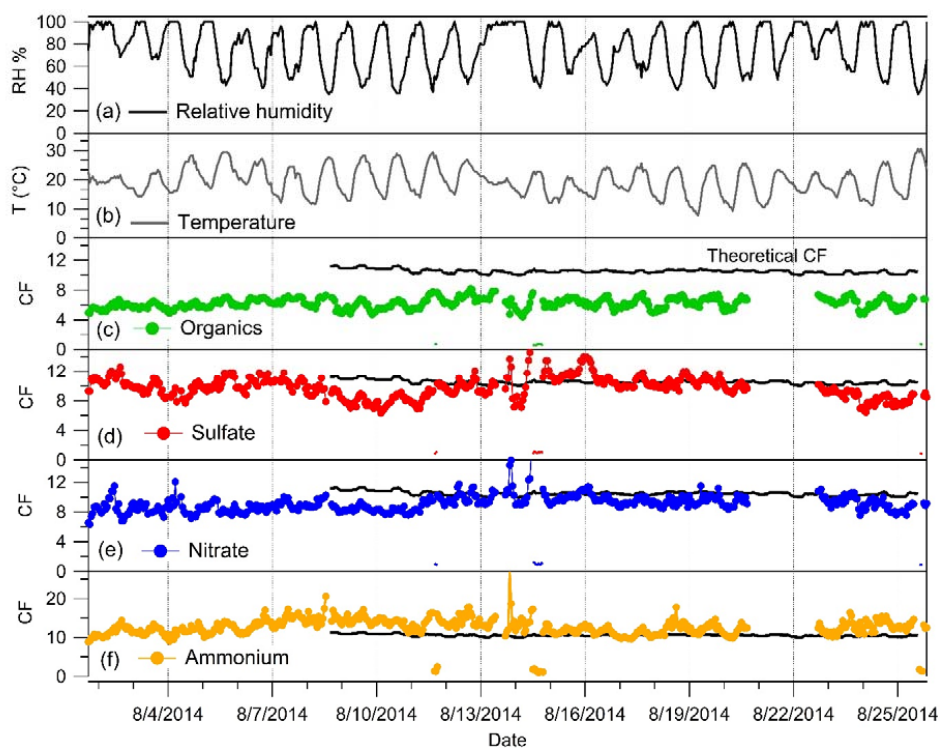
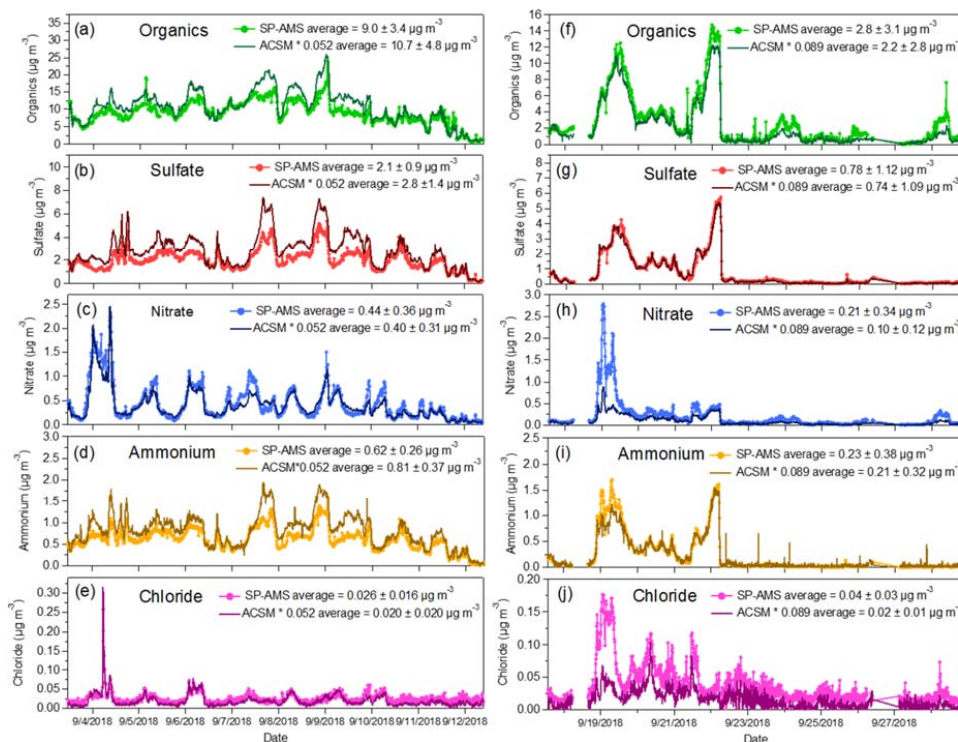
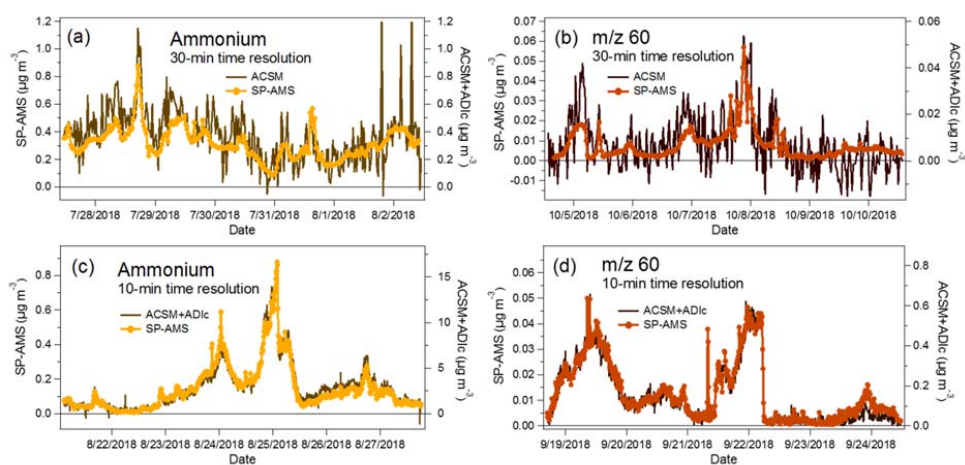


**Figure 7.** Ambient measurements at ARI showing ambient relative humidity (a), ambient  
615 temperature (b) and measured CFs for organics (c), sulfate (d), nitrate (e), and ammonium (f). The  
theoretical CF is shown with the black line in (c) – (f).



620 **Figure 8.** Ambient measurements at SMEAR III showing the mass loadings for organics (a, f), sulfate (b, g), nitrate (c, h), ammonium (d, i), and chloride (e, j) measured with the SP-AMS and the ACSM+ADIC in high flow (a–e) and low flow (f–j) regimes. ACSM+ADIC data was corrected for CF as described in the text.



625

**Figure 9.** Time series of ammonium and m/z 60 with 30-min time resolution with ACSM and SP-AMS (a-b) and 10-min time resolution with SP-AMS and ACSM+ADic (c)-(d) at SMEAR III

630